Thermal vibrational disorder of a conjugated polymer in charge-transfer complex

M. O. Osotov, V. V. Bruevich,[a] and D. Yu. Paraschuk[b]
Faculty of Physics and International Laser Center, M.V. Lomonosov Moscow State University, Moscow 119991, Russia

(Received 5 June 2009; accepted 11 August 2009; published online 3 September 2009)

Temperature dependences of optical absorption and Raman spectra of ground-state charge-transfer complex (CTC) formed in blends of a conjugated polymer, poly[2-methoxy-5-(2′-ethyl-hexyloxy)-p-phenylenevinylene] (MEH-PPV), and low-molecular-weight acceptor, 2,4,7-trinitrofluorenone, were studied. Upon cooling from 320 to 120 K, the polymer strongest Raman band shows a 0.5 cm^{-1} low-frequency shift while it demonstrates a 0.5 cm^{-1} high-frequency shift in the CTC. This behavior is explained by the temperature dependence of polymer-acceptor charge transfer in the CTC: The amount of transferred charge decreases by 25% upon cooling. At the same time, both the pristine polymer and CTC demonstrate a 0.05–0.1 eV redshift of the absorption edge. To account for these temperature shifts, we propose a model that relates temperature variations in the effective conjugation length with thermal torsion vibrations of the conjugated chains. Comparison of the model and experimental data reveals that the torsion rigidity of conjugated chains involved in the CTC is 30% stronger than that of the pristine ones. This enhanced rigidity increases the conjugation length of MEH-PPV chains in the CTC by 20%. However, the major contribution to the MEH-PPV absorption edge shift in the CTC is assigned to a local built-in electric field effect induced by the ground-state charge transfer. © *2009 American Institute of Physics*. [doi:10.1063/1.3216106]

I. INTRODUCTION

Blends of π-conjugated polymers (CPs) with various acceptors are actively studied as promising materials for organic solar cells and photodetectors. In the blends, a CP can form a ground-state charge-transfer complex (CTC) of the Mulliken type with some low-molecular-weight organic acceptors.[1,2] Moreover, recent studies on polymer-fullerene blends have revealed the presence of a ground-state CTC of the Mulliken type,[3] the fact that passed indiscernible in earlier studies.

The CTC formation can result in a profound effect on the optical and photophysical properties of the blend[4] as well as on its morphology.[5] poly[2-methoxy-5-(2′-ethyl-hexyloxy)-p-phenylenevinylene] (MEH-PPV)/2,4,7-trinitrofluorenone (TNF) CTC absorbs in the red and near IR where both the pristine donor and acceptor are transparent. The formation of CTC leads to shifts of the CP vibration frequencies of both the donor and acceptor.[6] Moreover, polymer conjugated segments seem to be significantly planarized in MEH-PPV/TNF CTC as was suggested from the Raman spectroscopy data.[7] The CTC formation could result in an increase of the conjugation length (CL) of the polymer and hence the corresponding redshift of its absorption edge. In fact, the main absorption band of MEH-PPV/TNF blend films does noticeably shift to the red relative to the pristine MEH-PPV; however, it was suggested that the CL increase does not give the major contribution to this shift.[7]

The Raman and absorption spectra of conjugated chains depend strongly on their conformation. As the chain conformation is highly sensitive to temperature, the temperature dependence of Raman, and absorption spectra should give more information on conformation of polymer conjugated segments involved in the CTC.

In this work, by studying temperature dependencies of optical absorption and Raman spectra of MEH-PPV/TNF blends, we analyze the conformation of conjugated segments involved in the CTC. The Raman spectroscopy is used to study the temperature dependence of the ground-state charge transfer from MEH-PPV to TNF. Using the optical absorption data, we investigate how the MEH-PPV properties are modified by the CTC. We propose a vibration disorder model (VDM) to associate the rigidity and planarity of the chain with the polymer CL. The model takes into account thermal torsion vibrations and is used to fit the experimental dependence of optical gap width on the temperature.

II. EFFECTIVE CONJUGATION LENGTH

The effective CL is known to be an important parameter determining the optical and electronic properties of a CP, and it is very sensitive to polymer's conformation. The CL depends on the degree of π-electron delocalization along the chain. The effective CL can be defined as the length of a model conjugated oligomer showing the same optical properties as the polymer. Obviously, the effective CL depends not only on the number of monomer units in the polymer but

[a]Electronic mail: bruevich@physics.msu.ru.
[b]Electronic mail: paras@polys.phys.msu.ru.

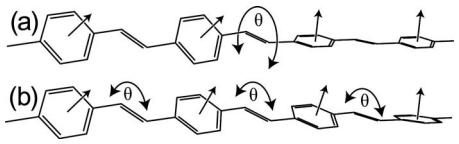

FIG. 1. Conjugation length confinement: abrupt flips (a) and conformational disorder (b).

rather on the density of conjugation defects. The CL of PPV-type polymers is generally evaluated as seven to ten monomer units.[8]

It is commonly accepted that the CL is limited mainly by chain's torsion deformations that decrease overlapping of neighboring π-orbitals.[9] Two different approaches were proposed to explain the conjugation confinement resulting from torsions: Abrupt flips model[10] and conformational disorder model.[11] Figure 1 illustrates these models. In the former, it is assumed that relatively plane conjugated segments are separated by random strong defects that break conjugation [Fig. 1(a)]. In the latter, the CL is limited by a weak disorder in torsion angles along the chain [Fig. 1(b)].

The advantage of the abrupt flip model is that one can easily construct the chain length distribution to describe the inhomogeneous broadening.[12] However, the optical absorption and photoluminescence data on MEH-PPV are better described by the conformational disorder model.[13]

III. VIBRATIONAL DISORDER MODEL

We present a VDM to describe the temperature evolution of CP optical gap. The model is based on the conformational disorder model introduced by Rossi *et al.*[11] The latter associates the CL with the correlation function between torsion angles by using a given torsional potential. In the VDM, we directly calculate the energy spectrum of a torsionally disordered conjugated chain using the Hückel method. The torsion amplitudes are calculated by using the quantum harmonic oscillator problem. This allows us to describe low-temperature vibrations dominated by zero-point fluctuations.

Assume that π-electron delocalization along the chain is limited by weak torsional disorder [Fig. 1(b)]. Consider a monomer unit as a rigid body. The orientation of the monomer unit is described by a vector [Fig. 1]. To describe torsions, we will use the simplest conjugated chain, i.e., that of *trans*-polyacetylene. Without torsions, the resonance integrals of the single and the double bonds are β_s and β_d, correspondingly. Allowing torsion around single bonds, the single bond resonance integral is $\beta_s(\theta)=\beta_s \cos\theta$,[11] where θ is the torsion angle between adjacent monomer units [Fig. 1(b)]. To calculate the optical gap of the torsionally disordered polyacetylene, we use the simplest Hückel molecular orbital method.[14] Assuming interaction only between neighboring monomer units, the torsion angles are independent of each other, and therefore we have

$$E_g - E_g^0 = 2\beta_s(1 - \langle \cos\theta \rangle), \tag{1}$$

where $E_g^0=2(\beta_d-\beta_s)$ is the bandgap of the torsionally ordered chain. The $\langle \cos\theta \rangle$ term is the average over all monomer units, and it contains the dependence of the optical gap on torsion defects.

Numerous optical studies of linear conjugated oligomers of different length indicate that their optical gap E_g scales with CL according to the Kuhn model:[15]

$$E_g = E_g^0 + \frac{\Delta E}{\mathrm{CL}}, \tag{2}$$

where CL is expressed in terms of a number of conjugated monomer units, and E_g^0, ΔE are fitting parameters. Note that the E_g^0 is the bandgap of infinite conjugated chain.

Assuming that the CL is limited only by torsions, from Eqs. (1) and (2) we obtain $\mathrm{CL} \propto 1/(1-\langle \cos\theta \rangle)$. In the case of small deviation from the equilibrium:

$$\mathrm{CL} \simeq \mathrm{const}/\langle \theta^2 \rangle. \tag{3}$$

Now include the CL temperature dependence in the model. Assuming the single torsional vibration with parabolic potential, the average torsion angle $\langle \theta^2 \rangle$ can be calculated by using the quantum harmonic oscillator model:

$$\langle \theta^2 \rangle \propto \sum_n \langle \theta^2 \rangle_n \exp\left(-\frac{h\omega(n+1/2)}{kT}\right), \tag{4}$$

where $\langle \theta^2 \rangle_n \propto n+1/2$ is the angular standard deviation of the nth vibration, ω is the oscillator angular frequency, k is the Boltzmann constant, and T is temperature. From Eqs. (3) and (4) we obtain

$$\mathrm{CL} = \mathrm{CL}_0 \tanh\left(\frac{\varepsilon}{2kT}\right), \tag{5}$$

where $\varepsilon=\hbar\omega$ is the characteristic energy of torsional vibrations, CL_0 is the CL at $T\to 0$. Note that even at $T\to 0$ the CL is finite due to zero-point oscillations. At high temperature, i.e., at $kT>\varepsilon$, the CL is limited mainly by thermal fluctuations.

Combining Eqs. (2) and (5), we have

$$E_g = E_g^0 + \Delta\tilde{E} \cdot \coth\left(\frac{\varepsilon}{2kT}\right), \tag{6}$$

where $E_g^0+\Delta\tilde{E}$ is the optical gap at $T\to 0$, and $\Delta\tilde{E} = \Delta E/\mathrm{CL}_0$. Equation (6) will be used to fit our experimental data. The optical gap in Eq. (6) is a sum of the temperature-independent (E_g^0) and temperature-dependent terms. The latter contains two parameters: The characteristic temperature change of the optical gap, $\Delta\tilde{E}$, and the characteristic energy that breaks conjugation, ε. As follows from the derivation of Eq. (6), the ε is associated with the force constant of torsion vibrations and hence with the torsion rigidity.

IV. EXPERIMENTAL

MEH-PPV and TNF were dissolved separately in chlorobenzene with concentrations in the range 2.5–5 g/l. Films were prepared by drop or spin casting (at 1000 rpm) on glass substrates from MEH-PPV:TNF solutions with molar ratios MEH-PPV:TNF ranging from 1:0.1 to 1:1 per MEH-PPV monomer unit. The samples were placed in an optical nitrogen-flow cryostat. The Raman spectrometer and mea-

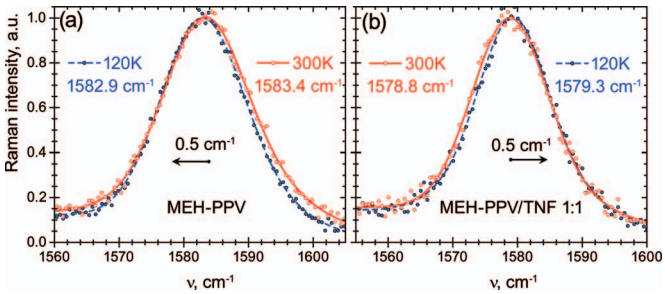

FIG. 2. The 1582 cm^{-1} Raman band in MEH-PPV (a) and 1:1 MEH-PPV:TNF (b) films at 120 and 300 K. The lines are guides to the eye. The arrows indicate the shift of the band maximum upon cooling.

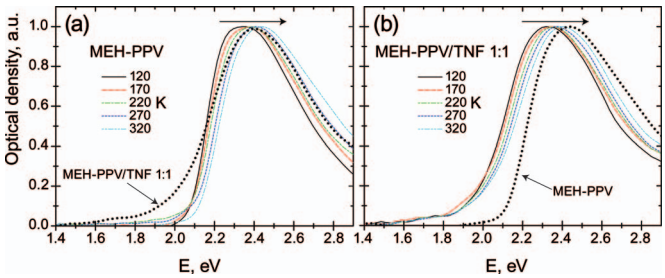

FIG. 3. Normalized absorption spectra of pristine MEH-PPV (a) and blend 1:1 MEH-PPV:TNF (b) films at various temperatures (curves). To compare the pristine and blend films, dots show the blend (a) and pristine (b) absorption spectra at 300 K. The arrows indicate the shift of the spectra upon heating.

surement details are described in Ref. 7. Briefly, the Raman spectra were recorded on drop-cast films by using a double monochromator DFS52 (LOMO) and thermoelectrically cooled photomultiplier R2949 (Hamamatsu). The external-cavity diode laser radiating at 670 nm was used for Raman excitation.[16] Instability in the laser wavelength gave the main contribution to the accuracy of determination of the Raman band wavenumbers. We repeated recording the Raman spectra until the accuracy of 0.1–0.2 cm^{-1} in the wavenumbers of the Raman band maximum was achieved.

Optical absorption spectra were measured on spin-cast films in the visible range using a monochromator MSD-4 (LOMO) equipped with a halogen lamp and silicon photodetector. The experimental details are described in Ref. 7. The optical gap of the films was measured at a level of 60% of the maximum optical density. This allowed us to maximize the experimental accuracy as this level corresponds to the maximum of the absorption spectrum derivative.

V. RESULTS

Figure 2 shows the 1582 cm^{-1} Raman band of MEH-PPV (a) and 1:1 MEH-PPV:TNF (b) films at two temperatures. The CTC formation between MEH-PPV and TNF leads to a frequency downshift of the strongest Raman band at 1582 cm^{-1}. This shift was assigned to a decrease in the π-electron density at the MEH-PPV conjugated backbone due to partial charge transfer from MEH-PPV to TNF.[6,7] Cooling down the pristine MEH-PPV film results in a frequency downshift of the 1582 cm^{-1} band by 0.5 ± 0.1 cm^{-1}. On the contrary, this band shows a frequency upshift by 0.5 ± 0.1 cm^{-1} in the blend. This opposite shift will be analyzed in the discussion section. The Raman band is somewhat narrowed upon cooling in both samples.

Figure 3 demonstrates normalized absorption spectra of pristine MEH-PPV and MEH-PPV:TNF films at various temperatures. Absorption of TNF starts at ~3 eV, and it is outside of the spectral range shown in Fig. 3. The characteristic changes of MEH-PPV absorption with addition of TNF are the appearance of a wide band extending down to near IR and a red shift of the MEH-PPV absorption band at 2.5 eV by about 0.2 eV [Fig. 3]. This intragap band was assigned to the ground-state MEH-PPV:TNF CTC.[1] Upon cooling, both the MEH-PPV and MEH-PPV:TNF spectra show red shifts of the main MEH-PPV absorption band. It is naturally to assign this shift to increasing the MEH-PPV CL (see Sec. VI).

Figure 4 plots temperature dependencies of the optical gap in the pristine polymer film and blends with different MEH-PPV:TNF ratios. The curves are fits by the VDM. The pristine and blend films show very similar temperature behavior. Cooling results in decreasing the optical gap that can be a signature of increasing the CL.

Table I shows the VDM parameters to fit to the experimental data in Fig. 4. The main (about 80%) contribution to the absorption shift in the CTC is associated with variation in the temperature-independent term of the VDM, E_g^0 [Eq. (6)]. Indeed, the curves in Fig. 4 shift vertically as a whole.

Interestingly, the parameter ε increases by $28 \pm 14\%$ in the CTC indicating higher torsional rigidity of the conjugated chains involved in the CTC. This increased rigidity results in a CL increase associated with decrease of torsions. However, the model shows that this increase contributes to the overall narrowing of the optical gap in the CTC only slightly (<20%), whereas the main contribution to that shift ensues from the change in E_g^0. This estimation has been made

TABLE I. Fitting parameters of the VDM for MEH-PPV and MEH-PPV:TNF films with different molar ratios. Figure 4 shows fitting curves.

	MEH-PPV:TNF molar ratio			
Fitting parameter	1:0	1:0.33	1:0.5	1:1
ε/k, K	450 ± 70	520 ± 30	580 ± 30	575 ± 3
$\Delta\tilde{E}$, eV	0.12 ± 0.03	0.150 ± 0.014	0.17 ± 0.02	0.164 ± 0.002
E_g^0, eV	2.05 ± 0.03	2.015 ± 0.013	1.988 ± 0.019	1.960 ± 0.002
$(E_g^0+\Delta\tilde{E})^a$ eV	2.166 ± 0.003	2.1650 ± 0.0010	2.1560 ± 0.0010	$2.124\ 47 \pm 0.00010$

[a]Optical gap at $T \to 0$.

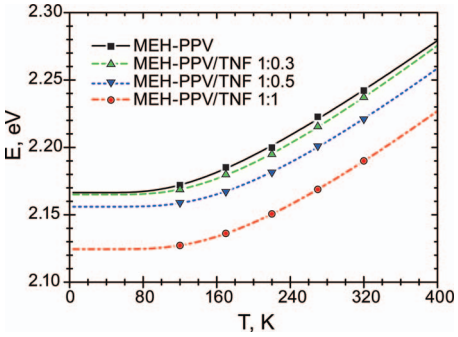

FIG. 4. Optical gap vs temperature in MEH-PPV and MEH-PPV:TNF films. Symbols are the experimental data, and curves are VDM fits with parameters given in Table I.

by substituting the values from Table I into the Eq. (6) and comparing the partial contributions of each parameter to the optical gap change upon CTC formation.

VI. DISCUSSION

A. Raman data

The strongest Raman band of pristine MEH-PPV at 1582 cm^{-1} assigned to the symmetric stretching vibration of the phenyl ring[17] shifts down upon cooling by 0.5 ± 0.1 cm^{-1}. A similar temperature shift was reported for another PPV-type polymer, BEH-PPV, and was assigned to increasing the effective CL.[18] Vibrational studies on PPV oligomers indicate that an increase in the oligomer length, i.e., in the CL, results in a downshift of the strongest Raman band.[19] The downshift was assigned to extension of conjugation between the phenylene and vinylene groups.

The CTC formation between MEH-PPV and TNF results in a 4 cm^{-1} frequency downshift of the strongest MEH-PPV Raman band at 1582 cm^{-1}.[6] This shift was assigned to depletion of the π-electron density at the polymer's backbone by $\sim 0.2e^-$ as a result of partial charge transfer from MEH-PPV to TNF in the electronic ground state.[6,7]

As follows from the absorption data, the effective CL both in the CTC and pristine polymer changes with temperature in a similar way. One might expect that cooling would result in a frequency downshift of the 1582 cm^{-1} Raman band in the CTC similar to the pristine MEH-PPV. On the contrary, we have observed the upshift. Consequently, the observed Raman upshift in the CTC upon cooling is not directly related to increasing the effective CL.

We suggest that the Raman upshift in the CTC is associated with reducing the charge-transfer degree upon cooling. The transferred charge upon MEH-PPV:TNF CTC formation is evaluated as $0.2e^-$ that corresponds to a 4 cm^{-1} downshift of the 1582 cm^{-1} MEH-PPV Raman band.[7] Therefore, the charge-transfer degree should be reduced by about 25% upon cooling that would result in a Raman upshift of 1.0 cm^{-1}. This upshift would overcompensate the 0.5 cm^{-1} Raman downshift resulting from increasing the CL.

Reducing the transferred charge upon cooling in the CTC can be explained as follows. According to the Mulliken model, the amount of transferred charge in the ground state is determined by the overlap integral between the donor highest occupied molecular orbital and the acceptor lowest unoccupied molecular orbital. This overlap integral depends nonlinearly on the nuclear coordinates modulated by thermal motion. This means that the averaged overlap integrals will depend on the amplitude of thermal motion. For example, assume that the overlap integral depends mainly on the donor-acceptor distance. It is naturally to suggest that the overlap integral decreases exponentially with the donor-acceptor distance. Therefore, the higher temperature, the larger the amplitude of thermal donor-acceptor vibrations and the higher the averaged overlap integral and the transferred electron density.

Thus, from the Raman studies, we suggest that cooling results in reducing the charge transferred from MEH-PPV to TNF in the electronic ground state. According to our experimental data, the amount of the transferred charge in the CTC is reduced by about 25% ($0.05e^-$) upon cooling by 200 K.

B. Absorption data

The absorption spectra of both the CTC and pristine polymer films shift to the red upon cooling (Figs. 3 and 4). The VDM (Sec. III) perfectly fits the experimental data (Fig. 4) for both the CTC and pristine polymer though the temperature dependence of charge transfer was not taken into account.

The Raman data indicate that the MEH-PPV:TNF CTC formation leads to planarization of conjugated segments involved in the CTC.[7] One may expect that planarization of the conjugated segments is accompanied by the decrease of their torsion deformation that limits the effective CL. Indeed, application of the VDM to our experimental data [Table I and Eq. (6)] shows that the torsional rigidity increases by $28 \pm 14\%$ in conjugated segments involved in the CTC as compared with the pristine ones. The resulting increase of the CL is approximately 20%. As noted in our previous study,[7] the planarization can be assigned to decrease in bending of the CTC conjugated segments; however, this bending might not affect the CL and optical gap noticeably.[20]

The main absorption band of MEH-PPV:TNF CTC is shifted noticeably to the red as compared to the pristine MEH-PPV. On the other hand, the torsional rigidity of the CTC conjugated chains and hence the effective CL is increased. It would seem that the absorption red shift could be assigned to the increase in the effective CL. However, the VDM indicates that the increased torsional rigidity (and hence the effective CL) contributes to the overall narrowing of the optical gap only slightly ($<20\%$). This supports our early suggestion that the main reason for the redshifted absorption in the CTC is not a change in the effective CL.[7] Otherwise, the increased CL should be explained by the enhanced torsion rigidity. Accordingly, the rigidity of the polymer chains is not improved enough in the CTC to explain the red shift in absorption.

Figure 5 illustrates how the E_g^0 could decrease in the CTC. Interchain interactions among polymer segments can result in the narrowing of the optical gap due to local field effects and Davydov splitting of the exciton absorption band [Fig. 5(b)]. The CTC formation is accompanied by appear-

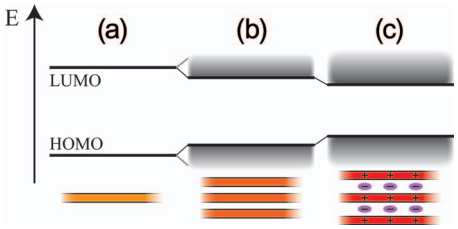

FIG. 5. Schematic of energy levels in single electron approximation (top) and conjugated chains (bottom) for chains: isolated (a), in film (b), and in CTC (c).

ance of a ground-state dipole [Fig. 5(c)]. Therefore, the interaction of chains with the local environment (including other chains) can be enhanced in the blended film. This may result in further narrowing of the optical gap [Fig. 5(c)]. Moreover, this permanent dipole generates a local electric field acting on the polymer chains. This field can result in a red shift of the main MEH-PPV absorption band as was observed in the electroabsorption spectroscopy studies of MEH-PPV films.[21] The characteristic electric field can be estimated from the amount of transferred charge $q=0.2e$ and a typical donor-acceptor distance of $r=0.35$ nm. This distance is typical for intermolecular interaction between the planes of the donor and acceptor conjugated molecules. As a result, the electric field strength should be about $F=q/4\pi\varepsilon_0 r^2 \simeq 2\cdot 10^7$ V/cm, where ε_0 is the electric constant. According to the electroabsorption data on MEH-PPV, the absorption edge shift in the applied electric field is $\Delta E \simeq F^2[\mathrm{V/cm}]10^{-14}$ eV.[21] Note that the built-in electric field is directed across the conjugated chains (Fig. 5) whereas their polarizability is highly anisotropic along the chains.[22] If we suppose that the angle between the built-in electric field and the chain is ~80°, then the observed absorption edge shift of ~0.1 eV can be explained by the built-in electric field.

VII. CONCLUSION

The effect of temperature on the Raman and absorption spectra of MEH-PPV:TNF CTC has been studied. We have observed that the strongest Raman band of MEH-PPV in the pristine film and CTC blended films shift in opposite directions upon cooling. If the temperature Raman shift in the pristine polymer is naturally explained by the change of its CL; in the CTC, the shift is accounted to the temperature dependence of charge transfer. At the same time, the main absorption band of MEH-PPV in both the pristine polymer and the CTC shifts similarly upon cooling. These shifts indicate that the effective CL changes similarly in both. We have developed a vibrational disorder model that associates the torsional deformation of conjugated chains with their effective CL and optical gap. The model excellently fits our experimental data indicating that the torsional rigidity of conjugated chains and their CL increase upon CTC formation. However, this change in the effective CL results only in a minor (~20%) contribution to the polymer absorption shift. On the other hand, the major contribution to the absorption edge shift in the CTC can be explained by electroabsorption in the local built-in electric field induced by the donor-acceptor ground-state charge transfer.

ACKNOWLEDGMENTS

The authors thank D. S. Martyanov for critical reading of this manuscript.

[1] A. A. Bakulin, A. N. Khodarev, D. S. Martyanov, S. G. Elizarov, I. V. Golovnin, D. Y. Paraschuk, S. A. Arnautov, and E. M. Nechvolodova, Dokl. Chem. **398**, 204 (2004).
[2] P. Panda, D. Veldman, J. Sweelssen, J. J. A. M. Bastiaansen, B. M. W. Langeveld-Voss, and S. C. J. Meskers, J. Phys. Chem. B **111**, 5076 (2007).
[3] J. J. Benson-Smith, L. Goris, K. Vandewal, K. Haenen, J. V. Manca, D. Vanderzande, D. D. C. Bradley, and J. Nelson, Adv. Funct. Mater. **17**, 451 (2007); K. Vandewal, A. Gadisa, W. D. Oosterbaan, S. Bertho, F. Banishoeib, I. Van Severen, L. Lutsen, T. J. Cleij, D. Vanderzande, and J. V. Manca, *ibid.* **18**, 2064 (2008); M. Hallermann, S. Haneder, and E. Da Como, Appl. Phys. Lett. **93**, 053307 (2008); T. Drori, C. X. Sheng, A. Ndobe, S. Singh, J. Holt, and Z. V. Vardeny, Phys. Rev. Lett. **101**, 037401 (2008).
[4] A. A. Bakulin, S. G. Elizarov, A. N. Khodarev, D. S. Martyanov, I. V. Golovnin, D. Y. Paraschuk, M. M. Triebel, I. V. Tolstov, E. L. Frankevich, S. A. Arnautov, and E. M. Nechvolodova, Synth. Met. **147**, 221 (2004).
[5] S. G. Elizarov, A. E. Ozimova, D. Y. Paraschuk, S. A. Arnautov, and E. M. Nechvolodova, Proc. SPIE **6257**, 293 (2006).
[6] D. Y. Paraschuk, S. G. Elizarov, A. N. Khodarev, A. N. Shchegolikhin, S. A. Arnautov, and E. M. Nechvolodova, JETP Lett. **81**, 467 (2005).
[7] V. V. Bruevich, T. S. Makhmutov, S. G. Elizarov, E. M. Nechvolodova, and D. Y. Paraschuk, J. Chem. Phys. **127**, 104905 (2007).
[8] B. Tian, G. Zerbi, R. Schenk, and K. Mullen, J. Chem. Phys. **95**, 3191 (1991); T. P. Nguyen, V. H. Tran, P. Destruel, and D. Oelkrug, Synth. Met. **101**, 633 (1999).
[9] J. L. Bredas, G. B. Street, B. Themans, and J. M. Andre, J. Chem. Phys. **83**, 1323 (1985).
[10] B. E. Kohler and I. D. W. Samuel, J. Chem. Phys. **103**, 6248 (1995).
[11] G. Rossi, R. R. Chance, and R. Silbey, J. Chem. Phys. **90**, 7594 (1989).
[12] S. G. Elizarov, Ph.D. thesis, Moscow State University, 2006.
[13] R. Chang, J. H. Hsu, W. S. Fann, K. K. Liang, C. H. Chang, M. Hayashi, J. Yu, S. H. Lin, E. C. Chang, K. R. Chuang, and S. A. Chen, Chem. Phys. Lett. **317**, 142 (2000).
[14] L. Salem, *The Molecular Orbital Theory of Conjugated Systems* (Benjamin, New York, 1966).
[15] H. Kuhn, J. Chem. Phys. **17**, 1198 (1949).
[16] V. V. Bruevich, S. G. Elizarov, and D. Y. Paraschuk, Quantum Electron. **36**, 399 (2006).
[17] F. H. Long, D. Mcbranch, T. W. Hagler, J. M. Robinson, B. I. Swanson, K. Pakbaz, S. Schricker, A. J. Heeger, and F. Wudl, Mol. Cryst. Liq. Cryst. **256**, 121 (1994).
[18] F. A. C. Oliveira, L. A. Cury, A. Righi, R. L. Moreira, P. S. S. Guimaraes, F. M. Matinaga, M. A. Pimenta, and R. A. Nogueira, J. Chem. Phys. **119**, 9777 (2003).
[19] A. Sakamoto, Y. Furukawa, and M. Tasumi, J. Phys. Chem. **96**, 1490 (1992).
[20] K. Becker, E. DaComo, J. Feldmann, F. Scheliga, E. ThornCsanyi, S. Tretiak, and J. M. Lupton, J. Phys. Chem. B **112**, 4859 (2008).
[21] M. Liess, S. Jeglinski, Z. V. Vardeny, M. Ozaki, K. Yoshino, Y. Ding, and T. Barton, Phys. Rev. B **56**, 15712 (1997).
[22] T. W. Hagler, K. Pakbaz, and A. J. Heeger, Phys. Rev. B **49**, 10968 (1994).